Non-Covalent Interactions: Complexes of Guanidinium with DNA and RNA Nucleobases

ARTICLE *in* THE JOURNAL OF PHYSICAL CHEMISTRY B · SEPTEMBER 2013

Impact Factor: 3.3 · DOI: 10.1021/jp407339v · Source: PubMed

THE JOURNAL OF PHYSICAL CHEMISTRY B

Article

pubs.acs.org/JPCB

Non-Covalent Interactions: Complexes of Guanidinium with DNA and RNA Nucleobases

Fernando Blanco,[†] Brendan Kelly,[‡] Goar Sánchez-Sanz,[§] Cristina Trujillo,[§] Ibon Alkorta,[∥] Jose Elguero,[∥] and Isabel Rozas*[,‡]

[†]Molecular Design Group, School of Biochemistry and Immunology, Trinity Biomedical Sciences Institute, University of Dublin, Trinity College, Trinity College, 152-160 Pearse Street, Dublin 2, Ireland

[‡]School of Chemistry, Trinity Biomedical Sciences Institute, Trinity College, Trinity College, 152-160 Pearse Street, Dublin 2, Ireland

[§]Institute of Organic Chemistry and Biochemistry, Gilead Sciences Research Center & IOCB, Academy of Sciences of the Czech Republic, Flemingovo nám. 2, 166 10 Praha 6, Czech Republic

[∥]Instituto de Química Médica, IQM-CSIC, Juan de la Cierva 3, 28006 Madrid, Spain

Supporting Information

ABSTRACT: Considering that guanidine-based derivatives are good DNA minor groove binders, we have theoretically studied, using the Polarizable Continuum model mimicking water solvation, the complexes formed by the biologically relevant guanidinium cation and the DNA and RNA nucleobases (adenine, guanine, cytosine, thymine, and uracil). The interactions established within these complexes both by hydrogen bonds and by cation−π interactions have been analyzed by means of the Atoms in Molecules and Natural Bond Orbital approaches. Moreover, maps of electron density difference have been produced to understand the cation−π complexes. Finally, the NICS and three-dimensional NICS maps of the cation−π complexes have been studied to understand the effect of the guanidinium cation on the aromaticity of the nucleobases.

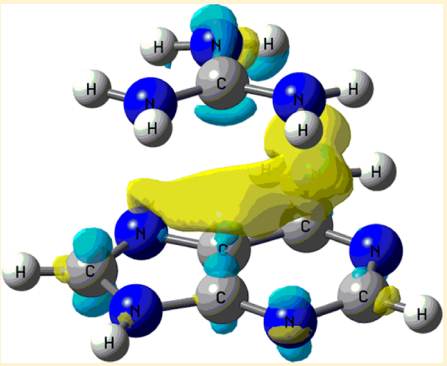

INTRODUCTION

The guanidinium cation is present in a large number of drugs clinically used such as guanabenz, an α_2-adrenoceptor agonist used as an antihypertensive,[1] the anticancer drug imatinib, which is a tyrosine kinase inhibitor developed by Ciba/Novartis,[2] or relenza one of the first commercialized anti-influenza virus agents.[3] The incorporation of this versatile group is fully justified by its ability to form a variety of interactions with the corresponding target due to hydrogen bond (HB) donation (two NH_2 and one NH) and to its positive charge. Hence, historically, it has been assumed that drugs containing guanidinium cations can form ionic interaction with negatively charged amino acids such as aspartate or glutamate and HBs with accepting groups such as those present in some amino acids and in the DNA and RNA bases. However, due to its planarity, resonance, and positive charge, the guanidinium cation can form other types of interactions, more in particular, cation−π interactions.[4−8]

Kerbale published in 1981 the first evidence of a cation−π interaction,[9] finding that benzene stabilizes K^+ ions in the gas phase better than in solvent. Since then, the experimental and computational study of this type of interaction has attracted a vast interest. For example, Meot-Ner established that also organic cations could act as good binders to benzene in the gas phase;[10] the analysis of 33 high-resolution protein crystals structures by Burley and Petsko showed that there is predisposition for cations to be in close proximity to aromatic rings,[11] and Flocco and Mowbray realized that the guanidinium group of Arg is arranged just directly over the center of the rings of aromatic amino acids more often than was expected.[12]

We have recently studied, at the theoretical level, the cation−π interactions established by the guanidinium cation and a series of simple aromatic organic systems such as benzene, naphthalene or pyridine;[4] we had also previously study the HB interactions formed by guanidinium and the (C═)O and (C═)N groups present in the RNA nucleic heterocyclic bases.[13] Considering that in the past years we have prepared several series of guanidinium containing derivatives that strongly interact with the minor groove of wild type DNA as well as with AT oligonucleotides,[14−19] in the present article, we aim to analyze the possible cation−π complexes formed between guanidinium and the aromatic systems present in the DNA and RNA bases (adenosine, guanidine, thymidine, cytosine, and uracil) with the final objective of understanding the DNA interactions previously observed by us and to complete our theoretical studies on guanidinium interactions.[20]

Received: July 24, 2013
Revised: August 28, 2013
Published: September 2, 2013

   dx.doi.org/10.1021/jp407339v | J. Phys. Chem. B 2013, 117, 11608−11616

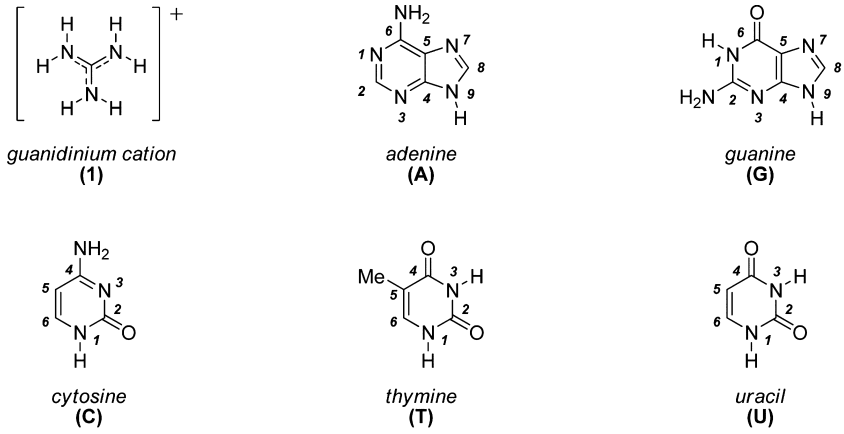

Figure 1. Structure and numbering of the systems involved in this study.

COMPUTATIONAL METHODS

All systems (monomers and complexes) have been optimized using the Gaussian09[21] package at the M05-2X[22] computational level with the 6-311+G(d,p)[23,24] basis sets. The M05-2X functional has been shown to properly describe weak interactions taking into account dispersion forces where other traditional functionals fail.[25] Frequency calculations have been performed at the same computational level to confirm that the resulting optimized structures are energetic minima. Effects of water solvation have been included by means of the SCFR-PCM approaches implemented in the Gaussian09 package including dispersing, repulsing, and cavitating energy terms of the solvent starting from the gas-phase geometries and reoptimizing. The interaction energy of the complexes in the present article has been calculated as the difference between the energy of the supermolecule and the sum of energies of the isolated monomers in their minimum energy configuration. Considering that all the calculations have been done using PCM (water solvent), the interaction energy cannot be corrected from the inherent basis set superposition error (BSSE).

The electron density of the complexes has been analyzed within the Atoms in Molecules (AIM) theory[26] using AIMAll[27] software. The Natural Bond Orbital (NBO) method[28] has been used to analyze the interaction of the occupied and unoccupied orbitals with the NBO-3 program,[29] since this kind of interaction is of utmost importance in the formation of hydrogen bonds and other charge transfer complexes.

The theoretical NICS values[30,31] were calculated using the GIAO[32,33] method on the optimized geometries. To calculate the spatial distribution of the NICS, its values have been calculated on a three-dimensional (3D) cubic grid of 12 Å side following the procedure described by Sánchez-Sanz et al.[34] The points in the grid are located 0.2 Å in the three spatial directions from each other. The result is a cube with 226981 NICS values that, in the next step, were represented within the electron density isosurface of 0.001 a.u. using the WFA program.[35]

RESULTS AND DISCUSSION

Structure and Energy. As previously mentioned, in a recent paper, we have studied the complexes formed between guanidinium and simple aromatic systems (benzene, naphthalene, and pyridine) in the gas phase and PCM−aqueous solvation obtaining only hydrogen-bonded complexes in the gas phase whereas using PCM−water different cation−π minima were localized. Accordingly, in this article, we extend this theoretical study to the complexes established by the guanidinium cation (**1**) and the five DNA/RNA nucleobases: adenine (A), guanine (G), cytosine (C), thymine (T), and uracil (U) (see Figure 1) using the M05-2X/6-311+G(d,p) level and the PCM−water approximation.

The molecular electrostatic potential (MEP) maps of the five nucleobases, shown in Figure 2, indicate that the lowest negative

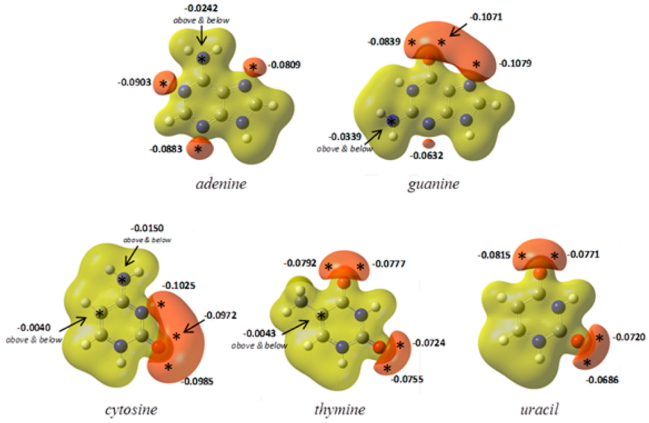

Figure 2. Representation of the MEP at the ±0.05 a.u. isosurface in the isolated nucleobases and the corresponding values and location of the MEP minima calculated at the M05-2X/6-311+G(d,p) level. Negative regions are represented in orange; positive regions are in yellow.

minima, as expected, are located near the N and O lone pairs. Adenine presents three main negative regions corresponding to the three N lone pairs (N1, N3, and N7), all in a similar range of MEP energies (−0.0903 to −0.0809 a.u.). The MEP of guanine shows a wide negative area comprising N7 and the two C═O lone pairs (−0.1079 to −0.0839 a.u.) and a second one corresponding to N3 where the value of the minimum is slightly lower (−0.0632 a.u.). In the case of cytosine, the MEP exhibit a large negative region, similar to that in guanine, corresponding to the overlapping of the adjacent N3 and C═O lone pairs, the absolute MEP minimum falling on N3 (−0.1025 a.u.). Finally, the MEPs of thymine and uracil (the most structurally related nucleobases) present identical patterns of MEP regions distributed on the C═O lone pairs with a narrow range of minima values (−0.0815 to −0.0686 a.u.) as it was previously pointed out by some authors.[36,37] Additional low MEP minima (<0.0500 a.u.) located on the perpendicular of the plane of the rings were found for four of the bases. These minima are

dx.doi.org/10.1021/jp407339v | J. Phys. Chem. B 2013, 117, 11608−11616

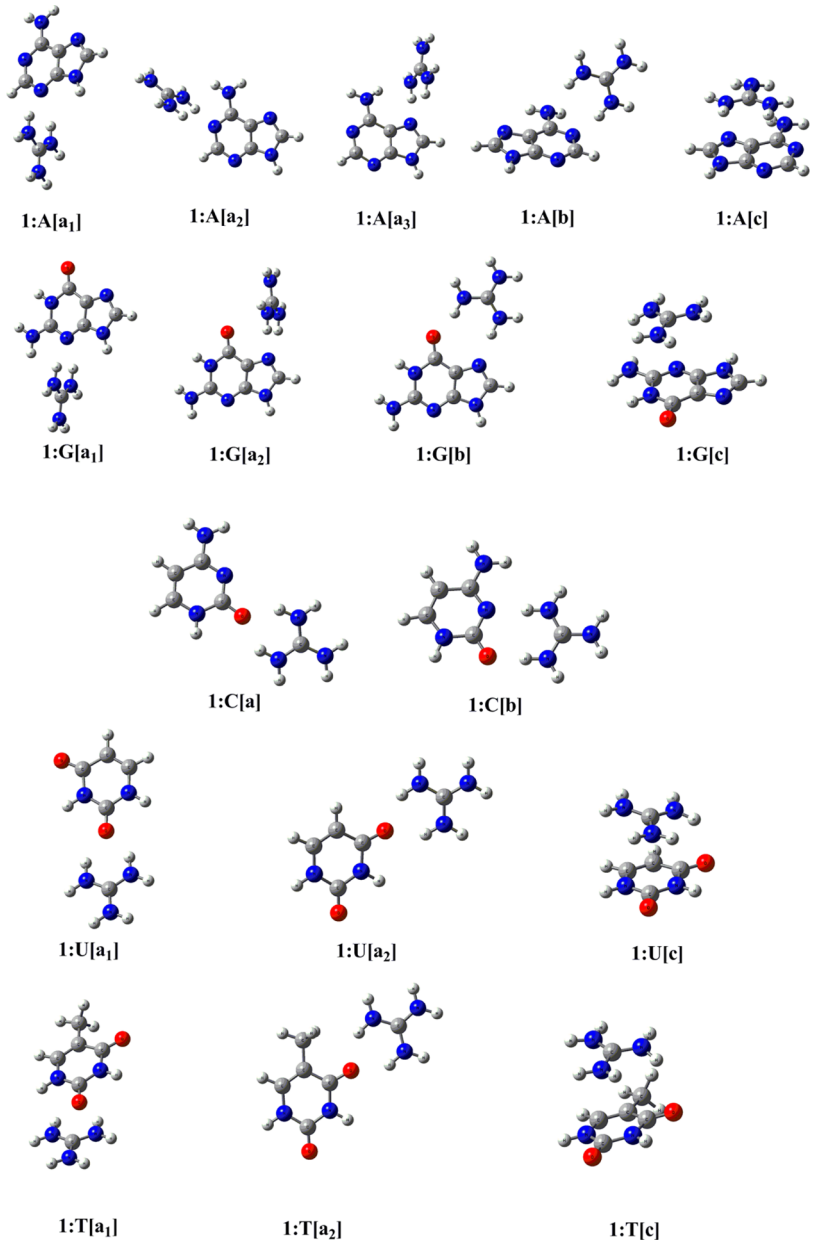

Figure 3. Optimized geometry of the complexes studied in this work at the M05-2X/6-311+G(d,p) level.

respectively placed on the amino groups for adenine, guanine, and cytosine and on C5 for cytosine and thymine.

A complete description of the dimers formed by the guanidinium cation and the five nucleobases is gathered in Figure 3. All the minima obtained correspond to different rearrangements involving HBs or cation−π interactions.

We have defined three main types of complexes based on the interactions established within: complex type [a] formed by a bifurcated HB between two guanidinium hydrogens and the lone pair(s) of a HB-acceptor atom (O or N) of the respective nucleobase; complex type [b] formed by a double HB interaction of two guanidinium hydrogens with the lone pairs of two adjacent HB-acceptor atoms (O or N) of the respective nucleobase; and complex type [c] formed by a cation−π interaction between the guanidinium system and the π cloud of the heteroaromatic rings of the respective nucleobase. Note that other geometries explored did not result in stable complexes, instead evolving to one of those shown in Figure 3.

Interaction energies (E_I), gathered in Table 1, show a clear prevalence of the HB complexes types [a] and [b] over type [c] for all the DNA/RNA bases, being the adenine complex **1:A**[**c**] the most stable of all cation−π complexes. Furthermore, in the case of cytosine, it was not possible to localize the stacked minimum [c] since it evolves to the highly stabilized complex **1:C**[**b**] where the guanidinium cation is involved in a double HB interaction with the adjacent carbonyl oxygen and pyrimidine nitrogen. A similar favorable arrangement is observed in the guanidine complex **1:G**[**b**], explaining its high stabilization compared to the corresponding type [$\mathbf{a}_{1,2}$] and [c] geometries (18.2−25.2 and 34.5 kJ mol^{-1}, respectively).

Uracil and thymine present a similar pattern of interaction energies, and the absolute minima correspond to the HB complexes **1:U**[$\mathbf{a}_2$] and **1:T**[$\mathbf{a}_2$], respectively, where the guanidinium moiety is interacting with the carbonyl groups on C4 (CO_{C4}), with a narrow energy difference from the **1:U**[$\mathbf{a}_1$] and **1:T**[$\mathbf{a}_1$] systems. It is well know that, in uracil, the O4 is more

dx.doi.org/10.1021/jp407339v | J. Phys. Chem. B 2013, 117, 11608−11616

Table 1. Interaction (kJ mol^{-1}) Energies of the Guanidinium−Nucleobase Complexes Studied at the M05-2X/6-311+G(d,p) Computational Level in PCM−Water Phase[a]

complex	E_I
1:A[a_1]	−24.3
1:A[a_2]	−25.7
1:A[a_3]	−26.5
1:A[b]	−42.4
1:A[c]	−8.2
1:G[a_1]	−22.0
1:G[a_2]	−29.1
1:G[b]	−47.3
1:G[c]	−2.8
1:C[a]	−39.1
1:C[b]	−48.2
1:U[a_1]	−29.8
1:U[a_2]	−31.6
1:U[c]	1.8
1:T[a_1]	−30.1
1:T[a_2]	−30.9
1:T[c]	−3.8

[a]All geometries of the complexes have C1 symmetry.

basic than the O2.[36−39] This result is consistent with the MEP minima values of CO_{C2} and CO_{C4} (Figure 1), slightly more favorable to CO_{C4}. The cation−π complexes **1:U**[c] and **1:T**[c] were rather unstable (E_I values: 1.8 and −3.8 kJ mol^{-1}).

These results seem to indicate that guanidinium interacts first by HBs with the nucleobases, in agreement with the only crystal structure solved for this type of guanidinium-based minor groove binders, the 4,4′-bis(2-aminoimidazolino)diphenylamine bound to an AT oligonucleotide.[40] In this structure can be observed how one NH of a 2-aminoimidazolinium cation (related to guanidinium) forms a bifurcated HB[41] with the O2 of a T and with the N3 of an A. It is interesting to note that, by looking at those complexes bound by cation−π forces, they are more stable with A and T than with any of the other nucleobases in agreement to the general tendency of these guanidinium-base minor groove binders to interact with the AT sequences present in the DNA minor groove.

Analysis of the Electron Density. The topological analysis of the electron density of the guanidinium complexes obtained indicates that a number of interactions (HBs and cation−π) are established with the nucleobases as shown by the bond critical points (BCP) detected in the graphical analysis (see some examples in Figure 4).

It needs to be pointed out that, since all the calculations have been carried out considering aqueous solvation, the properties of the interactions observed are somewhat "dumped" making the intermolecular bonding weaker that it would be in the gas phase. The BCPs, both for HB and cation−π interactions, present small values of the electron density (ρ_{BCP}) and positive Laplacian ($\nabla^2\rho$), as presented in Table S2 (Supporting Information), indicating the closed shell characteristics of the weak interactions established among the guanidinium and the nucleobases.[42] In general, HBs (N···H or O···H) show larger ρ_{BCP} values (10^{-2} a.u. order of magnitude) than those found in the cation−π interactions (10^{-3} a.u. order of magnitude).

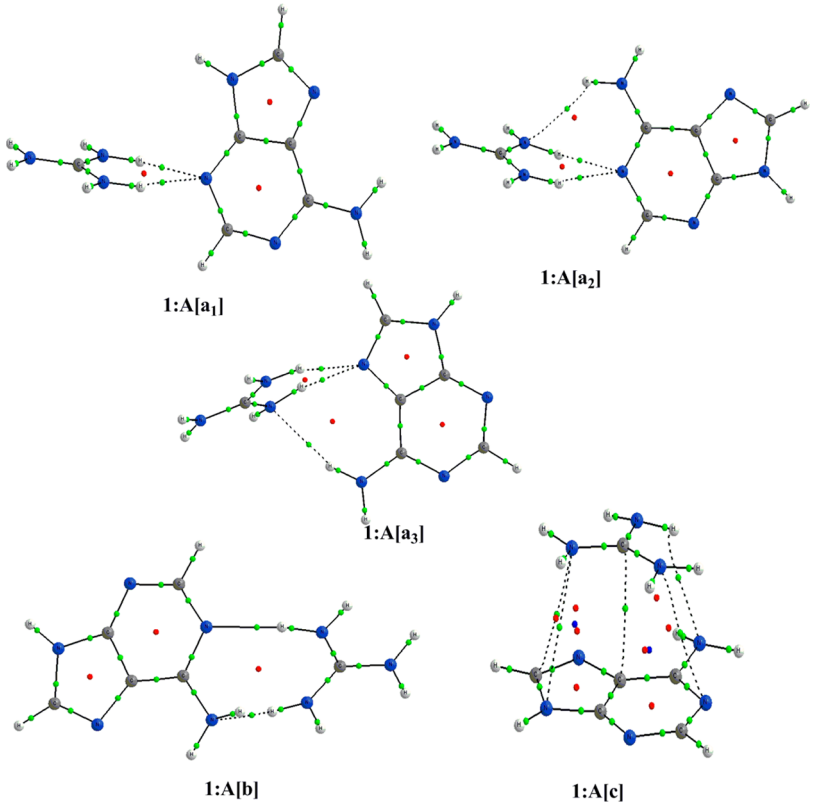

Figure 4. Molecular graph (AIM) of the hydrogen-bonded complexes **1:A**[a_1-a_3] and **1:A**[b] and the cation−π complex **1:A**[c] calculated at the M05-2X/6-311+G(d,p) computational level in PCM−water phase. Green, red, and blue balls indicate bond, ring, and cage critical points, respectively. (For interpretation of the references to color, the reader is referred to the web version of the article.)

dx.doi.org/10.1021/jp407339v | J. Phys. Chem. B 2013, 117, 11608−11616

In the case of **1:G[a2]**, which is a HB complex type, two orthogonal O···N interactions are found besides the expected HBs. In these pnictogen bonds, previously observed by some of us,[43] the O atom acts as a electron donor while the N behaves as an acceptor. Additionally, a number of ring and cage critical points (RCP and CCP, see Figure 4 for some examples) were found within these complexes. This type scenario has been previously reported by us and others.[44−46]

Among the variety of interactions established within these complexes (N···H, O···H, N···N, C···N, C···C, and O···N), we have found exponential relationships between the interatomic distances and the ρ_{BCP} for all the interactions except for O···N and C···C due to the lack of enough data to perform relevant fitting (Figure 5). The exponential relationships found present

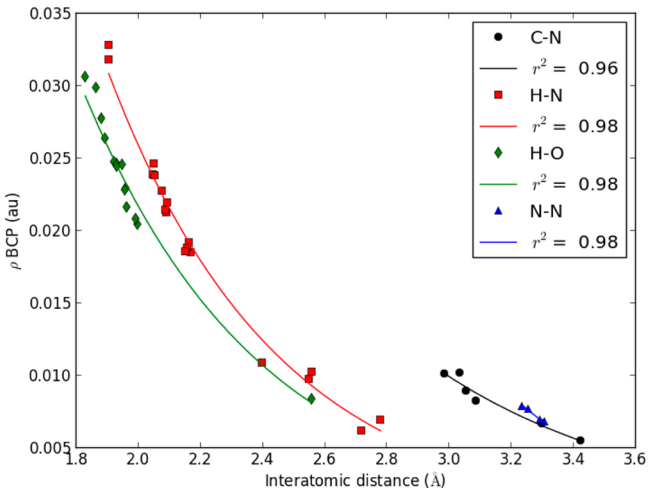

Figure 5. Relationships found between the interatomic distances (Å) and the value of the electron density at the BCP (a.u.) for the HB interactions.

good R^2 correlation coefficients: 0.96 for C···N; 0.98 for N···H, N···N, and O···H data. These relationships are in agreement with previous reports showing similar tendencies in the same and in other weak interactions.[47−53]

To achieve a visual description of the electronic displacement that results from the complexation process when compared to the electronic distribution in the isolated guanidinium and nucleobases, electron density difference maps have been calculated for the cation−π complexes **1A[c]**, **1G[c]**, **1T[c]**, and **1U[c]** (Figure 6).

Thus, the maps corresponding to the **1A[c]** complex show strong charge-depleting regions (yellow) on top of the nucleobases and small charge-gaining regions (light blue) under the guanidinium, in agreement with the relatively strong interaction energy observed in this complex (−8.2 kJ mol^{-1}). However, in the complexes **1T[c]** and **1G[c]**, the map exhibits a smaller depleting region that becomes even smaller in the corresponding **1U[c]** electron density difference map. This trend is in agreement with the lower stability of the corresponding complexes (−3.8, −2.8, and 1.8 kJ mol^{-1}, respectively). In all cases, the location of the depleting regions (yellow areas) in between both planes of the monomers suggests that the nucleobases are the ones losing electron density upon complexation with the guanidinium cation.

Natural Bond Orbital (NBO) Analysis. The NBO analysis of these complexes was carried out to assess the charge transferred and orbital interactions established, and the results

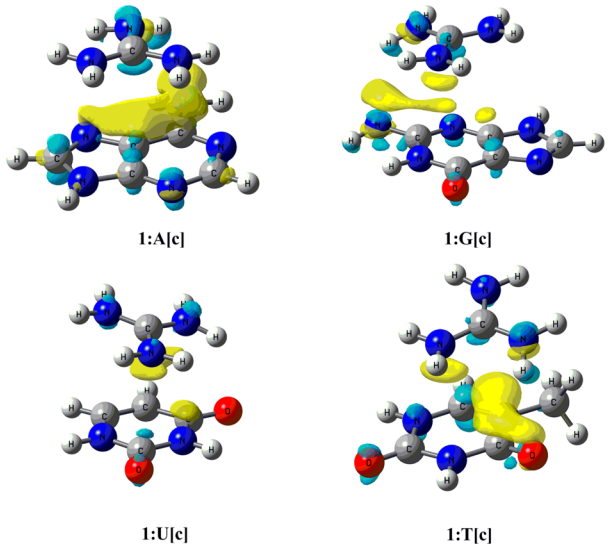

Figure 6. Electron density difference maps of the cation−π complexes form between guanidinium and four of the nucleobases (A, G, U, and T). Light blue and yellow isosurfaces represent gain and loss of electron density upon complexation with respect to the isolated subunits. Contours shown are 0.0005*e*/a.u. calculated at the M05-2X/6-311++G(d,p) level.

are presented in Table 2. The study of the NBO charges shows that, for cation−π interactions, none or insignificant charge transfer takes place in any direction, since the charge transferred was always less than 0.008. For the HB complexes, those of type [b] showed the largest transfer of charge between units with values up to 0.078*e*. These complexes involve two HBs between two heteroatoms interacting with the guanidinium as opposed to bifurcated HBs interacting with one heteroatom in complexes of type [a], the result being that complexes of type [b] accept more positive charge from guanidinium (≤0.078) than those of type [a] (≤0.044).

Those NBO second-order perturbation energy ($E(2)$) values larger than 4.2 kJ mol^{-1} are presented in Table 2. In the cation−π complexes, the most important orbital interactions are those from the C−C bonding orbitals of the aromatic systems to an "empty" lone pair of the guanidinium central C atom (BD CC → LP* C_G) indicating a donation from the aromatic system to guanidinium. Where an acceptor orbital is appropriately oriented, donation from a guanidinium N lone pair to antibonding orbitals on the nucleobase occur, such as BD* C^2N^3 ← LP N^{Gua} in **1:G[c]** and BD* C^2O ← LP N^{Gua} in **1:U[a2]**. In general, the magnitudes of the second-order perturbation energies are smaller in cation−π complexes than in HB complexes.

Moreover, complexes of type [b] have much higher $E(2)$ values than those of type [a] owing to the guanidinium having interactions with two electron donors instead of one, as is the case of [a] complexes. The strongest observed $E(2)$ values in [b] complexes correspond to donation from sp^2 hybridized aromatic N lone pairs to N−H antibonding orbitals of guanidinium (74.1−79.9 kJ mol^{-1}) being stronger than donations from the carbonyl O lone pairs (28.3−42.1 kJ mol^{-1}) or sp^3 hybridized N lone pairs (24.6 kJ mol^{-1}) with the same guanidinium N−H antibonding orbitals.

In type [a] complexes, the strongest orbital interactions also follow this preference, that is, the guanidinium N−H antibonding orbitals interacting with aromatic sp^2 N lone pairs.

dx.doi.org/10.1021/jp407339v | J. Phys. Chem. B 2013, 117, 11608−11616

Table 2. Orbital Energy [$E(2)$, kJ mol^{-1}], Orbital Interaction and Charge Transfer (e, Nucleobase → Guanidinium, Positive Values) of the Complexes Studied Here

complex	orbital interaction	$E(2)$	charge[a]
1:A[a$_1$]	BD N^3C^2 → BD* NH	4.4	0.008
	LP N^3 → BD* NH	**34.0**	
	LP N^3 → BD* NH′	16.3	
1:A[a$_2$]	LP N^1 → BD* NH	**41.0**	0.035
	LP N^1 → BD* NH′	24.2	
1:A[a$_3$]	BD N^7C^5 → BD* NH	4.8	0.027
	LP N^7 → BD* NH	**34.0**	
	LP N^7 → BD* NH′	17.2	
	BD* NH^{NH2} ← LP N^{gua}	9.3	
1:A[b]	LP N^{NH2} → BD* NH	24.6	0.055
	LP N^1 → BD* NH	**76.9**	
1:A[c]	BD C^5C^6 → LP* C^{gua}	**20.9**	0.008
1:G[a$_1$]	BD N^3C^2 → BD* NH	4.4	0.036
	BD N^3C^2 → BD* NH′	4.9	
	LP N^3 → BD* NH	**27.4**	
	LP N^3 → BD* NH′	23.7	
1:G[a$_2$]	LP N^7 → BD* NH	25.1	0.034
	LP N^7 → BD* NH′	**26.0**	
1:G[b]	LP N^7 → BD* NH	**79.9**	0.068
	LP^1 O → BD* NH	42.1	
	LP^2 O → BD* NH	28.3	
1:G[c]	BD C^2N^3 → LP* C^{gua}	**9.0**	0.005
	LP N^{NH2} → BD* NH	4.6	
	BD* C^2N^3 ← LP N^{gua}	5.8	
1:C[a]	LP^1 O → BD* NH	24.7	0.044
	LP^1 O → BD* NH′	22.9	
	LP^2 O → BD* NH	6.5	
	LP^2 O → BD* NH′	**32.0**	
1:C[b]	LP N^3 → BD* NH	**74.1**	0.078
	LP^1 O → BD* NH′	33.6	
	LP^2 O → BD* NH′	58.3	
1:U[a$_1$]	LP^1 O → BD* NH	**18.2**	0.028
	LP^1 O → BD* NH′	17.6	
	LP^2 O → BD* NH	16.4	
	LP^2 O → BD* NH′	8.8	
1:U[a$_2$]	LP^1 O → BD* NH	**20.4**	0.032
	LP^1 O → BD* NH′	20.0	
	LP^2 O → BD* NH	17.3	
	LP^2 O → BD* NH′	11.2	
1:U[c]	BD* C^2O ← LP N^{gua}	**4.4**	−0.006
1:T[a$_1$]	LP1 O → BD* NH	**20.4**	0.030
	LP1 O → BD* NH′	17.9	
	LP2 O → BD* NH	17.5	
	LP2 O → BD* NH′	9.3	
1:T[a$_2$]	LP1 O → BD* NH	16.6	0.032
	LP1 O → BD* NH′	22.3	
	LP2 O → BD* NH	**23.9**	
	LP2 O → BD* NH′	5.1	
1:T[c]	–	–	−0.000

[a]Charge transferred, calculated as the difference between the sums of the natural charges of each subunit.

Particularly, in purines A and G, these lone pairs interact with two of the guanidinium N−H antibonding orbitals simultaneously, one interaction being roughly twice as large due to proximity of the overlapping orbitals in the optimized geometries. In complexes with pyrimidinic bases (C, U, and T), the dominant interactions are always between the lone pairs of carbonyl O atoms and the guanidinium N−H antibonding orbitals. The geometry of these complexes allows both lone pairs to interact with each of the guanidinium N−H antibonding orbitals in bifurcated HBs, with relative strengths dependent on their separation.

The $E(2)$ energies from the NBO analyses strongly agree with the interaction energies of the optimized complexes. The strongest $E(2)$ values were seen for complexes of type [b], which are the most stable complex type for **1:A**, **1:G**, and **1:C**. In fact, a good logarithmic correlation was found between the corresponding E_I and the sum of all $E(2)$ values for each complex: $E_I = 21.03 \times \ln[E(2)] - 58.18$; $R^2 = 0.944$.

Aromaticity: NICS Calculation. In order to assess how the aromaticity on the nucleobases studied is affected upon cation−π complexation, the NICS values have been obtained. As it was previously show,[34] the NICS(0) may lead to spurious interpretation of the aromatic properties, since the proximity of the atom nuclei may distort the NICS values. Therefore, NICS(1) and NICS(2), which are the NICS values 1 and 2 Å above the center of the ring, were calculated. In the case of the purinic bases A and G, both the five- and six-member rings were considered.

The aromaticity of the nucleobases had been previously studied by several authors by calculating, for example, the HOMA and NICS indexes.[54] Since we want to assess the effect on aromaticity upon complexation, we have calculated the NICS of all the nucleobases as well as of the cation−π complexes with the same level of theory, and the results are summarized in Table 3. For comparison purposes, the benzene NICS values calculated at the same level of theory have been included.[34,55] Our results, in agreement with previous data found in the literature,[50] indicate that A is the only nucleobase that shows NICS values (the corresponding to the six-member ring) closed to those of benzene. The five-member ring presents large NICS values, similar to those found in the literature for pyrrole.[31,34] Similar results were found for the five-member ring in G.

In the complexes, the NICS values in the opposite face to the interaction have been calculated. Regarding the six-member ring, in A, the NICS values increase with respect to the isolated monomer (except NICS(2)). In G and its complexes, NICS(0) increases, and both NICS(1) and NICS(2) remains constant. In T and U, there is a decrease in the NICS values on the complexes, with the exception of T NICS(0), which is slightly larger. For the five-member rings, in A, NICS (0) and NICS(2) increase upon complexation, and the same occurs in G NICS(1), but the rest of NICS values decrease with respect to the isolated basis.

To get a more accurate view of the effect of the cation−π complexation on the aromaticity of the nucleobases, we have obtained the 3D NICS on the 0.001 a.u. electron density isosurface spatial representation of the isolated basis and their cation−π complexes (Figure 7). By comparing the isosurfaces of the isolated bases obtained with those of previous studies (benzene or pyridine),[34] it can be observed that A shows similar features. The rest of the nitrogen bases present isosurfaces that resemble more to non-aromatic compounds.

The NICS values on the 0.001 a.u. electron density isosurface for the cation−π complexes (Figure 7) reveal that, upon complexation, the NICS distribution in the surfaces remains very similar to that in the isolated monomers.

CONCLUSIONS

The complexes established by the guanidinium cation and the five nucleobases by means of cation−π and hydrogen-bonding

dx.doi.org/10.1021/jp407339v | J. Phys. Chem. B 2013, 117, 11608−11616

Table 3. NICS Values (ppm) on (0) and over (1, 2) the Ring Center for Nucleobases and Complexes at the M05-2X/6-311+G(d,p) Computational Level

	6-member ring			5-member ring		
	NICS(0)	NICS(1)	NICS(2)	NICS(0)	NICS(1)	NICS(2)
benzene	−7.4	−10.4	−5.1	–	–	–
adenine	−5.8	−8.6	−4.3	−10.9	−10.0	−4.3
thymine	−0.8	−2.0	−1.2	–	–	–
cytosine	−0.5	−3.0	−1.7	–	–	–
guanine	−2.3	−3.6	−2.1	−11.2	−9.6	−4.0
uracil	−0.3	−1.7	−1.0	–	–	–
1:A[c]	−6.6	−8.7	−4.2	−11.3	−9.8	−4.1
1:T[c]	−1.0	−1.9	−1.1	–	–	–
1:G[c]	−2.7	−3.6	−2.1	−10.9	−9.8	−3.9
1:U[c]	−0.1	−1.4	−0.9	–	–	–

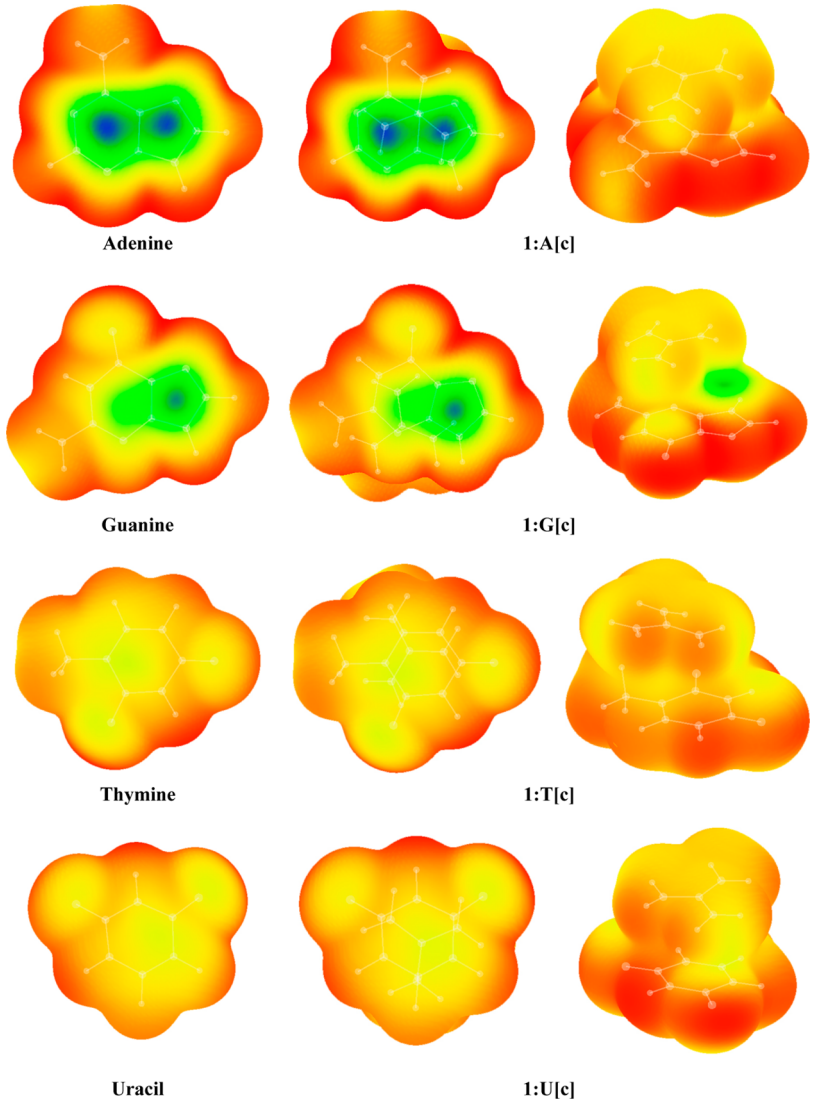

Figure 7. 3D representation of the NICS values (ppm) on the 0.001 a.u. electron density isosurfaces of adenine, guanine, thymine, and uracil and the cation−π guanidinium complexes studied at the M05-2X/6-311+G(d,p) computational level. Blue < −5.0; green > −5.0; yellow > −2.5; red > 0.0. 3D representation of the NICS values (ppm) on the 0.001 a.u. electron density isosurfaces NICS color scheme: Blue < −5.0; green > −5.0; yellow > −2.5; red > 0.0.

interactions have been theoretically studied using PCM−water at the M05-2X/6-311++G(d,p) level.

All the minima found corresponded to complexes of three different types: [a] formed by a bifurcated HB between two guanidinium hydrogens and the lone pair(s) of a HB-acceptor atom (O or N) of the nucleobase; [b] formed by a double HB interaction of two guanidinium hydrogens with the lone pairs of two adjacent HB-acceptor atoms (O or N) of the nucleobase;

dx.doi.org/10.1021/jp407339v | J. Phys. Chem. B 2013, 117, 11608−11616

and [c] formed by a cation−π interaction between the guanidinium system and the π cloud of the heteroaromatic rings of the nucleobase.

Considering the interaction energy, the most stable complexes found, for all the nucleobases, were the HB complexes types [a] and [b], and among the type [c], the most stable cation−π complex was that of adenine, **1:A[c]**.

The topological analysis of the electron density of these guanidinium complexes showed a number of interactions (HBs and cation−π) established with the nucleobases as shown by the critical points found. The electron density at the BCPs and Laplacian of the ρ_{BCP} are in agreement with weak interactions, being HBs in the [a] and [b] complexes and weaker than HB for the type [c] complexes. Different correlations were found between the interatomic distances and the value of the electron density at the BCP for the HB interactions.

The NBO analysis showed that, based on the perturbation energy $E(2)$, the most important bonding interactions in the HB complexes [a] and [b] were mostly from the lone pair of a heteroatom in a nucleobase to an antibonding N−H orbital of guanidinium (LP N/O → BD* NH). In the case of the [c] cation−π complexes, the most important bonding contribution was due to the interaction between a bonding C−C or C−N orbitals and the empty "lone pair" of the guanidinium central C. In all these complexes, a logarithmic correlation was found between the $E(2)$ and the interaction energy E_I.

Finally, to understand the effect that the complexation with a guanidinium cation has on the aromaticity of the nucleobases, the NICS(0), (1), and (2) were calculated, and the 3D NICS surfaces were produced, finding that only adenine and its complex show aromatic character that was not heavily modified upon complexation.

■ ASSOCIATED CONTENT

Supporting Information

Total energies of all complexes; interaction distance (Å), electron density at the bond critical point (a.u.), and Laplacian of this electron density (a.u.) of all the interactions established within the complexes studied; and full ref 21. This material is available free of charge via the Internet at http://pubs.acs.org.

■ AUTHOR INFORMATION

Corresponding Author

*Phone: (+353)18963731; fax: (+353)16712826; e-mail: rozasi@tcd.ie.

Author Contributions

The manuscript was written through contributions of all authors. All authors have given approval to the final version of the manuscript.

Notes

The authors declare no competing financial interest.

■ ACKNOWLEDGMENTS

This work was supported by the HEA-PRTLI-5 (BK), the European Commission (Marie-Curie grant, People FP7, project reference: 274988) (FB), the Ministerio de Ciencia e Innovación (project no. CTQ2012-35513-C02-02), and the Comunidad Autónoma de Madrid (project MADRISOLAR2, S2009/PPQ-1533) (GSS). Thanks are given to Dr. Martin Peters from ICHEC (Ireland), to the CTI (CSIC, Spain), and to the Centro de Computación Científica de la Universidad Autónoma de Madrid (Spain) for allocation of computer time.

■ REFERENCES

(1) Nash, D. T. Clinical Trial with Guanabenz, a New Antihypertensive Agent. *J. Clin. Pharmacol.* **1973**, *13*, 416−421.

(2) Buchdunger, E.; Zimmermann, J.; Mett, H.; Meyer, T.; Mueller, M.; Druker, B. J.; Lydon, N. B. Inhibition of the Abl Protein-Tyrosine Kinase in Vitro and in Vivo by a 2-Phenylaminopyrimidine Derivative. *Cancer Res.* **1996**, *56*, 100−104.

(3) GlaxoSmithKline. http://us.gsk.com/html/medicines/index.html (accessed June 29, 2013).

(4) Kelly, B.; Sanchez-Sanz, G.; Blanco, F.; Rozas, I. Cation−π *vs.* π−π Interactions: Complexes of 2-Pyridinylguanidinium Derivatives and Aromatic Systems. *Comp. Theor. Chem.* **2012**, *998*, 64−73.

(5) Carrazana-Garcia, J. A.; Rodriguez-Otero, J.; Cabaleiro-Lago, E. M. A Computational Study of Anion-Modulated Cation−π Interactions. *J. Phys. Chem. B* **2012**, *116*, 5860−5871.

(6) Cabaleiro-Lago, E. M.; Rodriguez-Otero, J.; Pena-Gallego, A. Effect of Microhydration on the Guanidinium···Benzene Interaction. *J. Chem. Phys.* **2011**, *135*, 214301−214309.

(7) Ryosuke, A.; Atsushi, H.; Tsutomu, A.; Shiraki, K. Arginine Increases the Solubility of Alkyl Gallates through Interaction with the Aromatic Ring. *Biochemistry* **2011**, *149*, 389−394.

(8) Crowley, P. B.; Golovin, A. Cation−π Interactions in Protein−Protein Interfaces. *Proteins* **2005**, *59*, 231−239.

(9) Sunder, J.; Nishizawa, K.; Kebarle, P. Ion-Solvent Molecule Interactions in the Gas Phase. The Potassium Ion and Benzene. *J. Phys. Chem.* **1981**, *85*, 1814−1820.

(10) Meot-Ner, M.; Deakyne, C. A. Unconventional Ionic Hydrogen Bonds. 2. $NH^+\cdots\pi$ Complexes of Onium Ions with Olefins and Benzene Derivatives. *J. Am. Chem. Soc.* **1985**, *107*, 474−479.

(11) Burley, S. K.; Petsko, G. A. Aromatic-Aromatic Interaction: A Mechanism of Protein Structure Stabilization. *Science* **1985**, *229*, 23−28.

(12) Flocco, M. A.; Mowbray, S. L. Planar Stacking Interactions of Arginine and Aromatic Side-Chains in Proteins. *J. Mol. Biol.* **1994**, *235*, 709−717.

(13) Rozas, I.; Alkorta, I.; Elguero, J. Modelling Protein−RNA Interactions: An Electron Density Study of the Guanidinium and Carboxylate Complexes with RNA Bases. *Org. Biomol. Chem.* **2005**, *3*, 366−371.

(14) Rodriguez, F.; Rozas, I.; Kaiser, M.; Brun, R.; Nguyen, B.; Wilson, W. D.; Garcia, R. N.; Dardonville, C. New Bis(2-aminoimidazoline) and Bisguanidine DNA Minor Groove Binders with Potent in Vivo Antitrypanosomal and Antiplasmodial Activity. *J. Med. Chem.* **2008**, *51*, 909−923.

(15) Nagle, P. S.; Rodriguez, F.; Kahvedžić, A.; Quinn, S. J.; Rozas, I. Non-Symmetrical Diaromatic Guanidinium/2-Aminoimidazolinium Derivatives: Synthesis and DNA Affinity. *J. Med. Chem.* **2009**, *52*, 7113−7121.

(16) Nagle, P. S.; Rodriguez, F.; Quinn, S. J.; O'Donovan, D. H.; Kelly, J. M.; Nguyen, B.; Wilson, W. D.; Rozas, I. Biophysical Studies on the DNA Interaction with Non-Symmetrical Guanidinium/2-Aminoimidazolinium Derivatives. *Org. Biomol. Chem.* **2010**, *8*, 5558−5567.

(17) Lopez, S.; McElhinney, R. S.; Margison, G. P.; McMurry, T. B. H.; Rozas, I. DNA Minor Groove Binding *O6*-Methylguanine-DNA Methyltransferase Inactivators. *Bioorg. Med. Chem.* **2011**, *19*, 1658−1665.

(18) Nagle, P. S.; Rodriguez, F.; Nguyen, B.; Wilson, W. D.; Rozas, I. High DNA Affinity of a Series of Amide Linked Aromatic Dications. *J. Med. Chem.* **2012**, *55*, 4397−4406.

(19) McKeever, C.; Kaiser, M.; Rozas, I. Aminoalkyl Derivatives of Guanidine Di-Aromatic Minor Groove Binders with Antiprotozoal Activity. *J. Med. Chem.* **2013**, *56*, 700−711.

(20) Rozas, I.; Sánchez-Sanz, G.; Alkorta, I.; Elguero, J. Solvent Effects on Guanidinium-Anion Interactions and Guanidinium Y-Aromaticity. *J. Phys. Org. Chem.* **2013**, *26*, 378−385.

(21) Frisch, M. J.; Trucks, G. W.; Schlegel, H. B.; Scuseria, G. E.; Robb, M. A.; Cheeseman, J. R.; Scalmani, G.; Barone, V.; Mennucci, B.; Petersson, G. A.; et al. *Gaussian 09*, Revision A.1; Gaussian, Inc.: Wallingford, CT, 2009.

(22) Zhao, Y.; Schultz, N. E.; Truhlar, D. G. Design of Density Functionals by Combining the Method of Constraint Satisfaction with Parametrization for Thermochemistry, Thermochemical Kinetics, and Noncovalent Interactions. *J. Chem. Theory Comput.* **2006**, *2*, 364−382.
(23) Ditchfield, R.; Hehre, W. J.; Pople, J. A. Self-Consistent Molecular-Orbital Methods. IX. An Extended Gaussian-Type Basis for Molecular Orbital Studies of Organic Molecules. *J. Chem. Phys.* **1971**, *54*, 724−728.
(24) Frisch, M. J.; Pople, J. A.; Binkley, J. S. Self-Consistent Molecular Orbital Methods 25. Supplementary Functions for Gaussian Basis Sets. *J. Chem. Phys.* **1984**, *80*, 3265−3269.
(25) Alkorta, I.; Blanco, F.; Elguero, J.; Dobado, J. A.; Ferrer, S. M.; Vidal, I. Carbon···Carbon Weak Interactions. *J. Phys. Chem. A* **2009**, *113*, 8387−8393.
(26) Bader, R. F. W. *Atoms in Molecules: A Quantum Theory*; Clarendon Press: Oxford, U.K., 1990.
(27) Keith, T. A. *AIMAll*, Version 11.04.03; TK Gristmill Software: Overland Park, KS, 2011; aim.tkgristmill.com.
(28) Reed, A. E.; Curtiss, L. A.; Weinhold, F. Intermolecular Interactions from a Natural Bond Orbital, Donor-Acceptor Viewpoint. *Chem. Rev.* **1988**, *88*, 899−926.
(29) Glendening, E. D.; Badenhoop, K.; Reed, A. E.; Carpenter, J. E.; Bohmann, J. A.; Morales, C. M.; Weinhold, F. *NBO 3.0*; Theoretical Chemistry Institute, University of Wisconsin: Madison, WI, 2001.
(30) Schleyer, P. v. R.; Maerker, C.; Dransfeld, A.; Jiao, H.; Hommes, N. J. R. v. E. Nucelus-Independent Chemical Shifts: A Simple and Efficient Aromaticity Probe. *J. Am. Chem. Soc.* **1996**, *118*, 6317−6318.
(31) Cyranski, M. K.; Krygowski, T. M.; Katritzky, A. R.; Schleyer, P. v. R. To What Extent Can Aromaticity Be Defined Uniquely. *J. Org. Chem.* **2002**, *67*, 1333−1338.
(32) Ditchfield, R. Self-Consistent Perturbation Theory of Diamagnetism. *Mol. Phys.* **1974**, *27*, 789−807.
(33) London, F. Theorie Quantique Des Courants Interatomiques Dans Les Combinaisons Aromatiques. *J. Phys. Radium* **1937**, *8*, 397−409.
(34) Sanchez-Sanz, G.; Trujillo, C.; Alkorta, I.; Elguero, J. A Theoretical NMR Study of the Structure of Benzynes and Some of Their Carbocyclic and Heterocyclic Analogs. *Tetrahedron* **2012**, *68*, 6548−6556.
(35) Bulat, F.; Toro-Labbé, A.; Brinck, T.; Murray, J.; Politzer, P. Quantitative Analysis of Molecular Surfaces: Areas, Volumes, Electrostatic Potentials and Average Local Ionization Energies. *J. Mol. Model.* **2010**, *16*, 1679−1691.
(36) Lamsabhi, A. M.; Alcamí, M.; Mó, O.; Yañez, M. Association of Cu^{2+} with Uracil and Its Thio Derivatives: A Theoretical Study. *ChemPhysChem* **2004**, *5*, 1871−1878.
(37) Trujillo, C.; Lamsabhi, A. M.; Mó, O.; Yañez, M.; Salpin, J.-Y. Interaction of Ca^{2+} with Uracil and Its Thio Derivatives in the Gas Phase. *Org. Biomol. Chem.* **2008**, *6*, 3695−3702.
(38) Eizaguirre, A.; Lamsabhi, A. M.; Mó, O.; Yáñez, M. Double Transfer in the Uracil Dimer Complex with Calcium. *Theor. Chem. Acc.* **2011**, *128*, 457−464.
(39) Trujillo, C.; Lamsabhi, A. M.; Mó, O.; Yáñez, M.; Salpin, J. Y. Unimolecular Reactivity of Uracil−Ca^{2+} Complexes in the Gas Phase. *Int. J. Mass Spectrom.* **2011**, *306*, 27−36.
(40) Glass, L. T. S.; Nguyen, B.; Goodwin, K. D.; Dardonville, C.; Wilson, W. D.; Long, E. C.; Georgiadis, M. M. Crystal Structure of a Trypanocidal 4,4′-Bis(Imidazolinylamino) Diphenylamine Bound to DNA. *Biochemistry* **2009**, *48*, 5943−5952.
(41) Rozas, I.; Alkorta, I.; Elguero, J. Bifurcated Hydrogen Bonds: Three-Centered Interactions. *J. Phys. Chem. A* **1998**, *102*, 9925−9932.
(42) Rozas, I.; Alkorta, I.; Elguero, J. Non-Conventional Hydrogen Bonds. *Chem. Soc. Rev.* **1998**, *27*, 163−170 and references therein.
(43) Sanchez-Sanz, G.; Trujillo, C.; Solimannejad, M.; Alkorta, I.; Elguero, J. Orthogonal Interactions between Nitryl Derivatives and Electron Donors: Pnictogen Bonds. *Phys. Chem. Chem. Phys.* **2013**, *15*, 14310−14318.
(44) Blanco, F.; Kelly, B.; Alkorta, I.; Rozas, I.; Elguero, J. Cation−π Interactions: Complexes of Guanidinium and Simple Aromatic Systems. *Chem. Phys. Lett.* **2011**, *511*, 129−134.
(45) Cubero, E.; Orozco, M.; Luque, F. J. A Topological Analysis of Electron Density in Cation−π Complexes. *J. Chem. Phys. A* **1999**, *103*, 315−321.
(46) Zhikol, O. A.; Shishkin, O. V.; Lyssenko, K. A.; Leszcynski, J. Electron Density Distribution in Stacked Benzene Dimers: A New Approach towards the Estimation of Stacking Interaction Energies. *J. Phys. Chem.* **2005**, *122*, 144104−144112.
(47) Alkorta, I.; Elguero, J. Fluorine−Fluorine Interactions: NMR and AIM Analysis. *Struct. Chem.* **2004**, *15*, 117−120.
(48) Tang, T. H.; Deretey, E.; Knak Jensen, S. J.; Csizmadia, I. G. Hydrogen Bonds: Relation between Lengths and Electron Densities at Bond Critical Points. *Eur. Phys. J. D* **2006**, *37*, 217−222.
(49) Vener, M. V.; Manaev, A. V.; Egorova, A. N.; Tsirelson, V. G. QTAIM Study of Strong H-Bonds with the O−H···A Fragment (A = O, N) in Three-Dimensional Periodical Crystals. *J. Phys. Chem. A* **2007**, *111*, 1155−1162.
(50) Mata, I.; Alkorta, I.; Molins, E.; Espinosa, E. Universal Features of the Electron Density Distribution in Hydrogen-Bonding Regions: A Comprehensive Study Involving H···X (X=H, C, N, O, F, S, Cl, π) Interactions. *Chem.—Eur. J.* **2010**, *16*, 2442−2452.
(51) Zeng, Y.; Li, X.; Zhang, X.; Zheng, S.; Meng, L. Insight into the Nature of the Interactions of Furan and Thiophene with Hydrogen Halides and Lithium Halides: Ab Initio and QTAIM Studies. *J. Mol. Model.* **2011**, *17*, 2907−2918.
(52) Sanchez-Sanz, G.; Alkorta, I.; Elguero, J. Theoretical Study of the HXYH Dimers (X, Y= O, S, Se). Hydrogen Bonding and Chalcogen-Chalcogen Interactions. *Mol. Phys.* **2011**, *109*, 2543−2542.
(53) Sanchez-Sanz, G.; Trujillo, C.; Alkorta, I.; Elguero, J. Intermolecular Weak Interactions in HTeXH Dimers (X=O, S, Se, Te): Hydrogen Bonds, Chalcogen−Chalcogen Contacts and Chiral Discrimination. *Chem. Phys. Chem.* **2012**, *13*, 496−503.
(54) Among others: (a) Kiralj, R.; Ferreira, M. M. C. On Heteroaromaticity of Nucleobases. Bond Lengths as Multidimensional Phenomena. *J. Chem. Inf. Comput. Sci.* **2003**, *43*, 787−809. (b) Huertas, O.; Poater, J.; Fuentes-Cabrera, M.; Orozco, M.; Sola, M.; Luque, F. J. Local Aromaticity in Natural Nucleobases and Their Size-Expanded Benzo-Fused Derivatives. *J. Phys. Chem. A* **2006**, *110*, 12249−12258. (c) Sun, G.; Nicklaus, M. C. Natural Resonance Structures and Aromaticity of the Nucleobases. *Theor. Chem. Acc.* **2007**, *117*, 323−332. (d) Cysewski, P.; Szefler, B. Environment Influences on the Aromatic Character of Nucleobases and Amino Acids. *J. Mol. Model.* **2010**, *16*, 1709−1720.
(55) De Proft, F.; Schleyer, P. v. R.; van Lenthe, J. H.; Stahl, F.; Geerlings, P. Magnetic Properties and Aromaticity of *o*-, *m*-, and *p*-Benzyne. *Chem.—Eur. J.* **2002**, *8*, 3402−3410.